Cracking caused by cutting of plasma-sprayed hydroxyapatite coatings and its relation to the structural features of coatings deposited at different initial substrate temperatures

Bojan R. Gligorijević[1], Miroljub N. Vilotijević[2,3], Maja J. Šćepanović[4], Radovan V. Radovanović[5], Nenad A. Radović[6]

[1]*University of Belgrade, Innovation Center of Faculty of Technology and Metallurgy, Belgrade, Serbia*
[2]*University of Belgrade, Vinča Institute of Nuclear Sciences, Belgrade, Serbia*
[3]*Plasma Jet Co, Belgrade, Serbia*
[4]*Center for Solid State Physics and New Materials, Institute of Physics, University of Belgrade, Zemun, Serbia*
[5]*Academy of Criminalistic and Police Studies, Belgrade, Serbia*
[6]*University of Belgrade, Faculty of Technology and Metallurgy, Department of Metallurgical Engineering, Belgrade, Serbia*

Abstract

The present study estimated the cracking phenomenon in as-plasma-sprayed hydroxylapatite coatings (HACs) after they were being subjected to the severe cutting conditions in the direction perpendicular to the coating/substrate interface. In order to evaluate the effects of substrate preheating on the occurrence of micro-cracks, the HACs were deposited at different initial substrate temperatures (T_S = 20, 100 and 200 °C). The changes in phase composition and HA splat morphology with T_S were observed and were correlated with the cracking occurrence. The results showed that severe cutting conditions introduced a localized cracking in the regions of HACs dominantly attributed to the brittle hydroxyl-deficient amorphous calcium phosphate (ACP) phase. This effect was particularly observable in the HACs deposited without preheating of substrate. On the other hand, the preheating of substrate reduced the presence of micro-cracks and caused insignificant changes in the average local phase composition. In HACs deposited with preheating of substrate, the HA splats (of which HACs are composed) were thinner and recrystallized HA regions seemed smaller in size and more evenly distributed. These results implied potentially important roles of the HA splat formation mechanism on the distribution of ACP and recrystallized HA regions in the as-plasma-sprayed HACs and the cracking resistance of HACs.

Keywords: plasma spraying, hydroxyapatite coatings, stress, cracking, substrate preheating.

Available online at the Journal website: http://www.ache.org.rs/HI/

SCIENTIFIC PAPER

UDC 621:533.9:66.069.832.09

Hem. Ind. **71** (3) 241–249 (2017)

Many studies have indicated that the mechanical integrity of plasma-sprayed HACs in terms of the bonding strength (cohesion and adhesion) is of critical importance when these coatings are applied on the surface of biomedical implants, such as titanium alloy, stainless steel, etc. [1–9]. Considering the fact that the plasma-sprayed HACs are composed of many individual building blocks known as „HA splats“ [2,8,10], it is evident that the properties of the splat-substrate and splat-splat interfaces will generally affect the bonding strength of HACs. Saber-Samandary *et al.* have discussed that „it is the first layer of splats which determines the coating-substrate adhesion, while the coating cohesion is determined by the nature of the intersplat contact [8].

One of the effective ways for enhancement of splat-substrate and intersplat contacts (or bonding strength of HACs) is the substrate preheating. Most of the previous studies have shown the beneficial effects of the substrate preheating on the bonding strength of HACs [4,7]. However, other opinions exist [6], as well. It has been shown that preheating of substrate may promote: *i*) the recrystallization in HACs [4,8], *ii*) the formation of thinner HA splats [8] and *iii*) the change in thermal and residual stresses in HACs [6,7]. Morks and Kobayashi have emphasized the brittle nature of the amorphous calcium phosphate (ACP) phase [4]. In this regard and taking into account the statement of Saber-Samandari *et al*. about the nature of the intersplat contact [8], two neighboring amorphous HA splats should exhibit a minimum resistance towards the propagation of cracks.

In the present study, the last hypothesis was tested. Namely, if as-plasma-sprayed HACs are subjected to

Correspondence: B.R. Gligorijević, University of Belgrade, Innovation Center of Faculty of Technology and Metallurgy, Karnegijeva 4, 11120 Belgrade, Serbia.
E-mail: bgligorijevic@tmf.bg.ac.rs; bojan.gligorijevic@gmail.com
Paper received: 13 May, 2016
Paper accepted: 30 August, 2016
https://doi.org/10.2298/HEMIND160513034G

the severe stress condition, such as cutting by using the handsaw, then the cracking of coating's scale should occur and should be preferentially localized within the ACP regions. The HACs deposited at different initial substrate temperatures (T_S) were severely cut to qualitatively observe the effects of the substrate preheating on the cracking occurrence. In addition, the changes in the phase composition and splat morphology with T_S were analysed and were correlated with the cracking phenomenon.

EXPERIMENTAL

Feedstock powder and substrate material

The substrate material was in the form of plates with dimensions of 25 mm×50 mm×3 mm. The plates were made of the implantation grade biomedical steel (AISI 316 LVM).

A commercially available HAP with particle size of 33 μm (XPT-D-703, Sulzer Metco, USA) was used for deposition of HACs. The particle size of HAP was listed according to manufacturer's data sheets. The morphology of the feedstock HAP was observed by using the scanning electron microscopy (SEM) coupled with energy dispersive spectrometry (EDS). The composition of HAP was confirmed by using the EDS, X-ray fluorescence (XRF) spectrometry, and micro-Raman spectroscopy (MRS).

Atmospheric plasma spraying

The HAP was deposited onto the steel substrates by using the high power laminar plasma spray process (Plasma Jet Co, Serbia) [7,9]. Prior to deposition process, the steel plates were sand-blasted with 2 mm Al_2O_3 particles and cleaned in ultrasonic bath. The steel plates were then placed on a vertical disk with 200 mm in diameter. During the deposition process, the disk was rotating at ~3.7 rev/s. The deposition of HAP was performed in two to three short intervals (7–10 s each) with pauses of few minutes between cycles. The HACs were deposited at different initial substrate temperatures T_S = 20, 100 and 200 °C. Other parameters were kept constant during the plasma deposition process (Table 1). Other details related to deposition process are given in Refs. [7,9].

Table 1. Plasma deposition parameters (PJ-100 installation)

Parameter	Value
Plasma power, kW	52.0±1.5
Plasma voltage, V	120±2
Plasma current, A	430±5
Argon flow (plasma forming gas), dm^3/min	38.5±1.2
Stand-off distance (*SOD*)	100 mm
Nitrogen flow (plasma forming gas), dm^3/min	28.2±1.0
Air flow (HAP carrier gas), dm^3/min	8.0
Powder mass input, g/s	2.0±0.1

Characterization of HACs

In order to introduce the cracking of the coating's scale, the HACs were cut in the direction depicted in Figure 1a by using a handsaw. Subsequently, the samples were hot-mounted in the bakelite resin with carbon filler (5.0±0.5 bar, 100±10 °C, 20±5 min). After hot-mounting, the cross-sections were ground with SiC water-proof abrasive papers (P-80, P-100, P-220, P-400, P-600, P-800, P-1000, P-1200, P-1500 and P-2000) and polished with Al_2O_3 water-based suspensions down to 1 μm. Other details related to sample preparation are given in Ref. [9].

Afterwards, the cross-sectional morphology of HACs was evaluated by using the SEM-EDS measurements, which were performed on a JEOL JSM–6610LV SEM coupled with Oxford Instruments X-Max SDD EDS (University of Belgrade, Faculty of Mining and Geology). During the analysis, the electron acceleration voltage of 20 kV and the tungsten filament were used. Prior to SEM-EDS analysis, the samples were coated with graphite particles in a vacuum chamber of a sputter coater device. The molar Ca/P ratio was measured along the thickness of HACs in steps of 5 μm by using the EDS line-scan analysis.

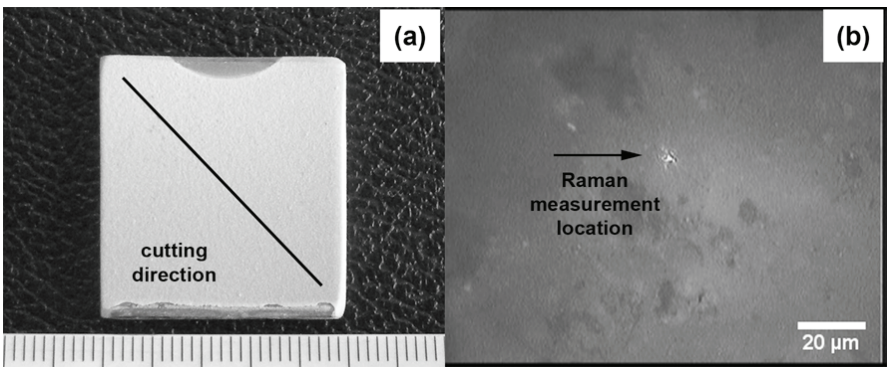

Figure 1. Macrograph of typical as-plasma-sprayed HAC (a) and typical micrograph of HAC's cross-section under the Raman microscope (b).

After SEM-EDS, re-polished cross-sections of HACs were examined by using the MRS (Figure 1b). Raman scattering measurements were performed in a back--scattering micro-Raman configuration using Jobin Yvon T64000 triple spectrometer (gratings with ~1800 grooves/mm), equipped with a confocal microscope, an x-y-z microscope stage and nitrogen cooled CCD detector. The Raman spectra were excited by the ~514.5 nm line of Coherent Ar^+/Kr^+ mixed laser, with output power of ~50 mW. The spectral resolution of the Raman system was ~2 cm^{-1}. The spectra were collected at room temperature in air, using 10× magnification objectives, with exposure time of 400 s. All spectra were calibrated against the strongest Raman band of polished Si wafer (~520.6 cm^{-1}). In the case of each HAC, the Raman measurements were performed in the same region of the cross-section and within the same range of distances from the coating/substrate interface (100–150 μm).

In order to observe the morphology of HA splats, the HACs were cut in the direction shown in Figure 1a by using the diamond saw. Afterwards, the samples were: *i*) cold mounted in acrylic compound, *ii*) ground by using the SiC water-proof abrasive papers (P-800, P-1200 and P-2000) and *iii*) polished with Al_2O_3 water--based suspensions down to 1 μm. The micro-structural properties of cross-sections of HACs were then analysed by using the inverted light microscope (LM) in the brigth field mode (Reichert-Jung MEF3). Prior to analysis, the polished cross-sections were chemically etched in the ~0.058 mol/l HNO_3 water solution. For each HAC, the etching time was 4–5 s. Considering the substantial difference between the solubility of the ACP and HA [11,12], the chemical etching was performed to reveal the distribution of ACP and recrystallized HA regions on the cross-sections of HACs, *i.e*., to delineate boundaries of HA splats.

RESULTS AND DISCUSSION

Feedstock powder (MRS, SEM-EDS)

When the HA powders of smaller sizes (20–45 μm) are deposited by using the atmospheric plasma spray process, they produce an enhanced lamellar structure of HA coatings in contrast to HA powders of larger sizes (75–125 μm) in which case the lamellar structure is barely distinguishable [13]. Therefore, the differences in morphology of HA splats formed from the HA powders of smaller sizes, introduced by preheating of substrate, can be more easily distinguished and evaluated compared to the HA splats formed from the HA powders of larger sizes. For this reason, the feedstock HA powder of relatively smaller size was used in the present study.

Figure 2a shows the spherical shape of the feedstock powder used in the present study. It should be

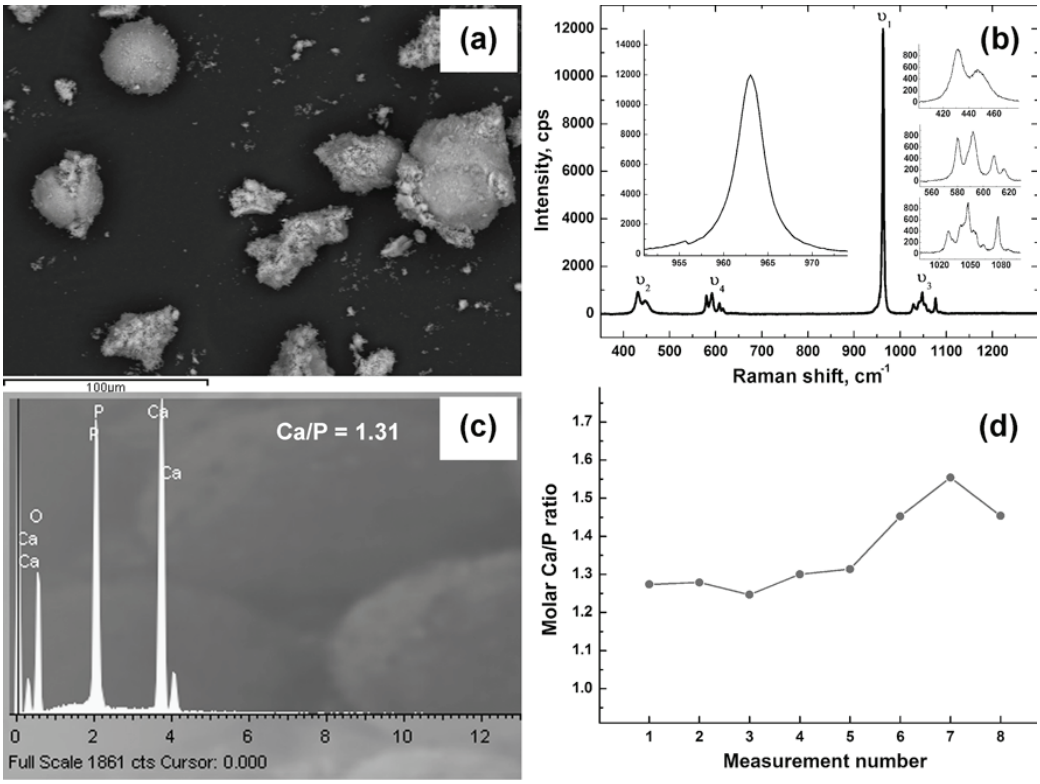

Figure 2. The SEM micrograph (a), MRS spectrum (b), EDS spectrum (c) and variation of molar Ca/P ratio (EDS analysis) (d) of the HA feedstock powder.

noted here that this figure represents the morphological appearance of the feedstock powder. In the present study, the determination of the feedstock powder size was not performed. The size of the feedstock powder was guaranteed by the manufacturer. The MRS analysis of the feedstock powder showed the presence of vibration modes of the phosphate group (PO_4^{3-}, Figure 2b) typically observed in HA powders [9,14,15]: *i*) O–P–O bending mode (ν_2), *ii*) O–P–O bending mode (ν_4), *iii*) P–O symmetric stretching mode (ν_1) and *iv*) P–O asymmetric stretching mode (ν_3). The OH^- bands detected at ~3572 cm^{-1} are not presented in Figure 2b. On the other hand, the EDS analysis of the feedstock powder (Figure 2c) showed the values of the molar Ca/P ratio roughly between 1.3 and 1.6 (Figure 2d). This result implied that initial HA feedstock powder was probably calcium-deficient (non-stoichiometric). The Ca/P mole ratio of the stoichiometric HA is ~1.667.

As a result of the thermal decomposition of HA feedstock powder in the high temperature plasma jet [15], the HACs may contain impurity phases with Ca/P mole ratios as follows [16]: *i*) α- and β-tricalcium phosphate (α- and β-TCP, Ca/P = 1.5), *ii*) oxyapatite/oxyhydroxyapatite (OA/OHA, Ca/P = 1.67), *iii*) tetracalcium phosphate (TTCP, Ca/P = 2.0), *iv*) calcium oxide (CaO, (Ca/P = ∞) and *v*) amorphous calcium phosphate (ACP, (Ca/P range 1.2–2.2). In the present study, the estimation of α-TCP, β-TCP, and OA/OHA presence in deposited HACs based on the the Ca/P mole ratio was uncertain because the Ca/P mole ratios for these phases overlap with the observed Ca/P mole ratio for HAP (1.3–1.6, Figure 2d). The only phases that may show distinctively different Ca/P mole ratio are ACP (1.2–2.2), TTCP (2.0) and CaO (∞). Although the EDS analysis cannot unambiguously differentiate between these phases, the higher Ca/P mole ratio in HACs may indicate their presence. Such information is relevant, considering that phases with higher Ca/P mole ratio (ACP, CaO and TTCP) form as a result of the most intensive thermal decomposition of the initial HA powder particles in the plasma jet [15,17].

Cracking occurrence and distribution of Ca/P mole ratio (SEM-EDS)

The SEM results showed that severe handsaw cutting introduced substantial presence of micro-cracks within the HACs deposited without preheating of substrate (T_S = 20 °C, Figure 3). Although not presented, it is noteworthy of mentioning that diamond-saw cutting of the same HAC samples produced only a small presence of vertical micro-cracks. The amount of stress introduced by handsaw cutting was much higher com-

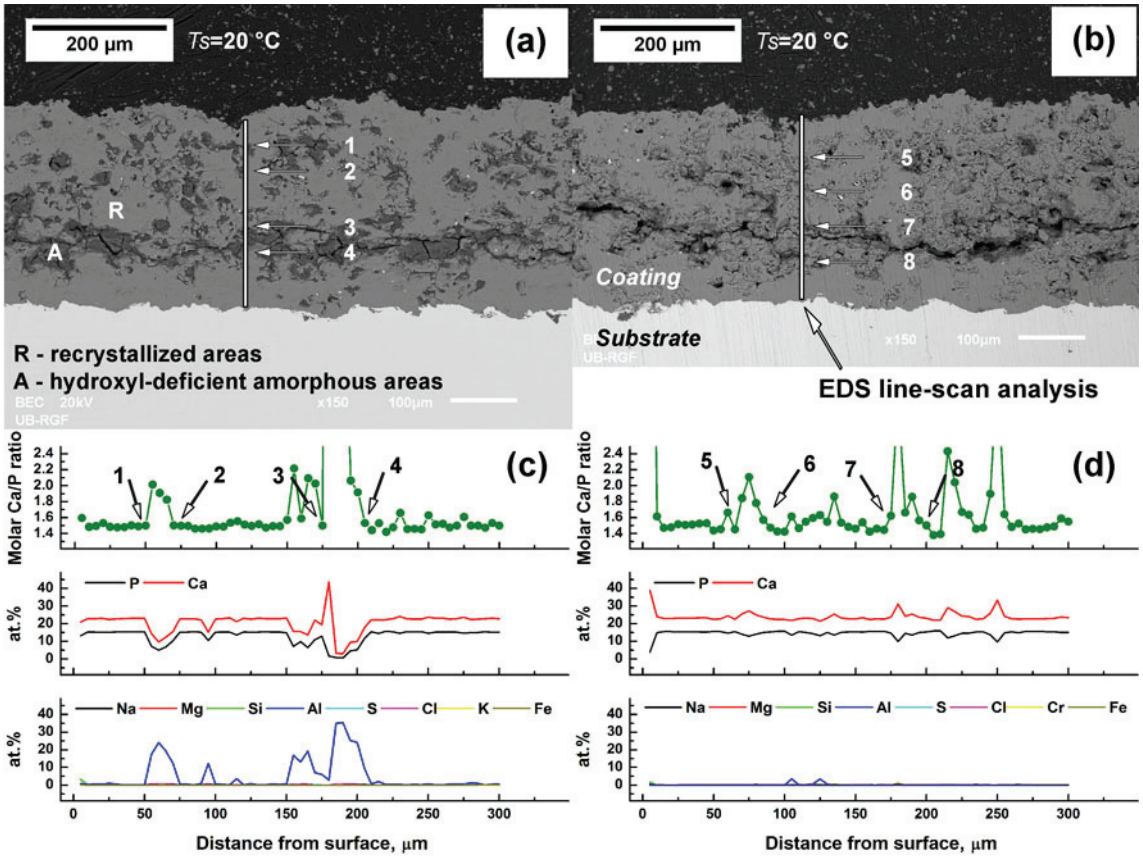

Figure 3. Polished (a) and grinded (b) cross-section of HAC deposited at T_S = 20 °C and corresponding EDS line-scan analyses (c and d). 1-2, 3-4, 5-6, and 7-8 represent the areas with increased Ca/P mole ratio.

pared to diamond-saw cutting. Figure 3a shows the polished cross-section of these HACs with two distinctive regions. The first region, with a rough surface, was filled with micro-cracks (designated with „A“ in Figure 3a), whereas the second region, with a flat surface, was free of micro-cracks (designated with „R“ in Figure 3a). The EDS measurements showed a minor presence of sodium (Na), magnesium (Mg), silicon (Si), sulphur (S), chlorine (Cl), potassium (K) and iron (Fe) (<0.2 at.%) (Figure 3c). On the other hand, increased amounts of aluminium (Al) were detected within the crack-containing regions. Considering that the presence of Al was undetected in the feedstock HA powder (Figure 2c and d), it was assumed that the increased amounts of Al detected on the cross-sections of HACs were related to the presence of Al_2O_3 particles used for polishing of cross-sections. Namely, due to their small size, the Al_2O_3 particles from water-based suspensions have probably filled the cracks and craters on cross-sections of HACs during the polishing stage. In Figure 3c, it is evident that distribution of Ca, P, and Ca/P changed accordingly to distribution of Al. In order to determine whether these changes were affected by the presence of Al_2O_3 particles, the cross-section of HAC shown in Figure 3a was ground for several seconds by SiC water-proof abrasive paper (P-2000) to remove the Al_2O_3 particles. After grinding, the cross-section was examined by the EDS line-scan analysis on the approximately same location. According to Figure 3d, the Ca and P distributions were affected by the Al_2O_3 presence. On the other hand, by comparing the EDS analysis between 1 and 2 (and 3 and 4, Figure 3a and c) with corresponding analysis between 5 and 6 (and 7 and 8) (Figure 3b and d), the presence of Al_2O_3 particles did not significantly affect the distribution of the Ca/P mole ratio along the thickness of HAC.

The EDS measurements showed that the Ca/P mole ratio changed roughly between 1.4 and 1.7 within the crack-free regions (Figure 3c), whereas this ratio was >1.8 within the crack-containing regions. The variations of the Ca/P mole ratio within the crack-free regions were close to the variations detected in the initial HA feedstock powder (Figure 2d). For this reason, these regions were attributed to the recrystallized HA (designated with „R“ in Figure 3a). On the other hand, the size of the crack-containing regions was much larger than the size of the initial HA feedstock powder. Thus, these regions could not be attributed to the thermally decomposed unmelted or partially molten HA particles of the initial HA feedstock powder. In fact, the cross-sectional examination of HACs showed that the initial HAP particles were nearly fully molten in the plasma jet (the unmelted or semi-molten HA particles of the initial HA feedstock powder could not be observed). For this reason, the crack-containing regions and, thus, an increased Ca/P mole ratio within these regions, were attributed to the hydroxyl-deficient ACP which probably contained CaO and TTCP (designated with „A” in Figure 3a). It is known that periphery of the molten HA particle may be overheated in the plasma jet [17]. The overheating causes the evaporation and loss of P_2O_5 and, consequently, an increase of the Ca/P mole ratio [17]. Only ~4.4 wt.% change in the phosphate content is sufficient to cause the crystallization of CaO and TTCP from the dephosphorized portion of the melt [17]. When such melt is rapidly cooled upon the impact of molten HA particle onto the substrate or prior-formed HA deposit, the resulting structure will be hydroxyl-deficient ACP phase inside which CaO and TTCP phases may co-exist. In previous study of Hesse *et al.* [18], the XRPD analysis have shown the relation between the ACP, CaO and TTCP contents. According to their results, the decrease in the ACP content, which is the highest in the interface area due to the highest cooling conditions, has followed the decrease in the CaO and TCP contents. These results are analogous to the results of the line-scan EDS analysis of HAC's cross-sections, presented in the review article of Surmenev [19], which has shown an increase in the Ca/P mole ratio in the near-interface region of HACs due to a presence of most intensively decomposed products of HA phase in the high-temperature plasma jet.

Further analysis showed that preheating of substrate at T_S = 100 °C noticeably reduced cracking of the coating's scale caused by the handsaw cutting (Figure 4a). When substrate was preheated at T_S = 200 °C, the cracking was almost imperceptible (Figure 4b). On the other hand, according to EDS-line-scan analyses presented in Figure 4c and d, the preheating of substrate insignificantly affected the variation of the Ca/P mole ratio (at least within the investigated T_S range). Although the crack-containing regions were nearly absent when substrates were preheated at T_S = 200 °C (Figure 4b), the variations in the Ca/P mole ratio indicated that the presence of the impurity phases was unchanged (Figure 4d).

HA splats morphology and cross-sectional microstructure (LM and MRS)

Figure 5a–c show chemically etched cross-sections of HACs deposited at different T_S. The darkest sphereical-like and/or ellipsoid-like objects were identified as pores. The recrystallized HA regions (light regions) were unetched and were intercepted with chemically etched ACP regions (darker regions). It is clear from Figure 5b and c that recrystallized HA regions appeared thinner and finer compared to that in Figure 5a. This result implied that preheating of substrate caused the formation of thinner HA splats. The recrystallized HA regions were smaller in size and more evenly dispersed in HACs

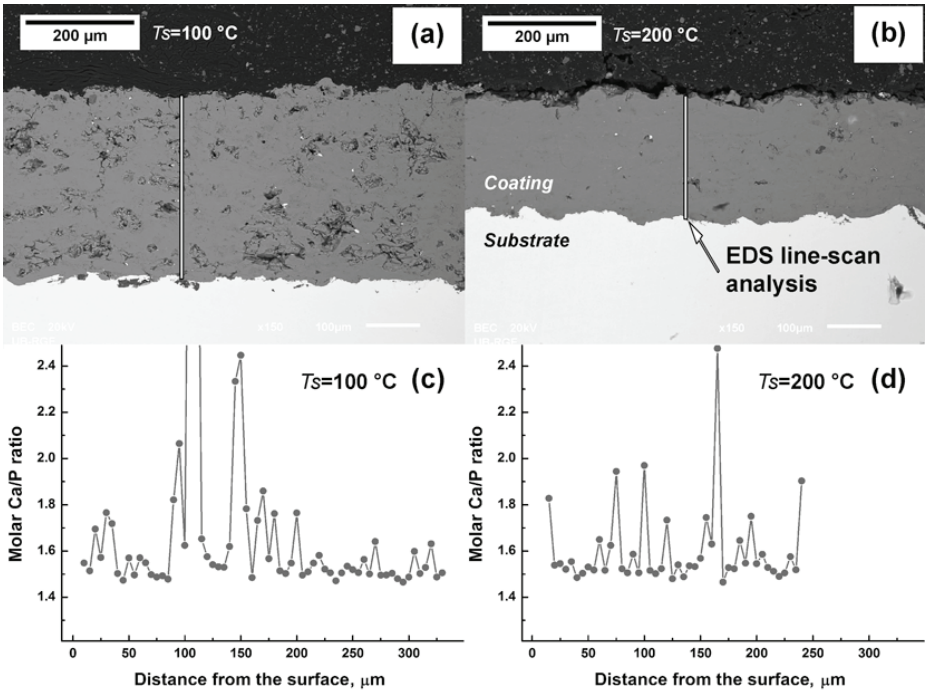

Figure 4. Polished cross-sections of HAC deposited at T_S = 100 (a) and 200 °C (b) and corresponding EDS line-scan analyses (c and d).

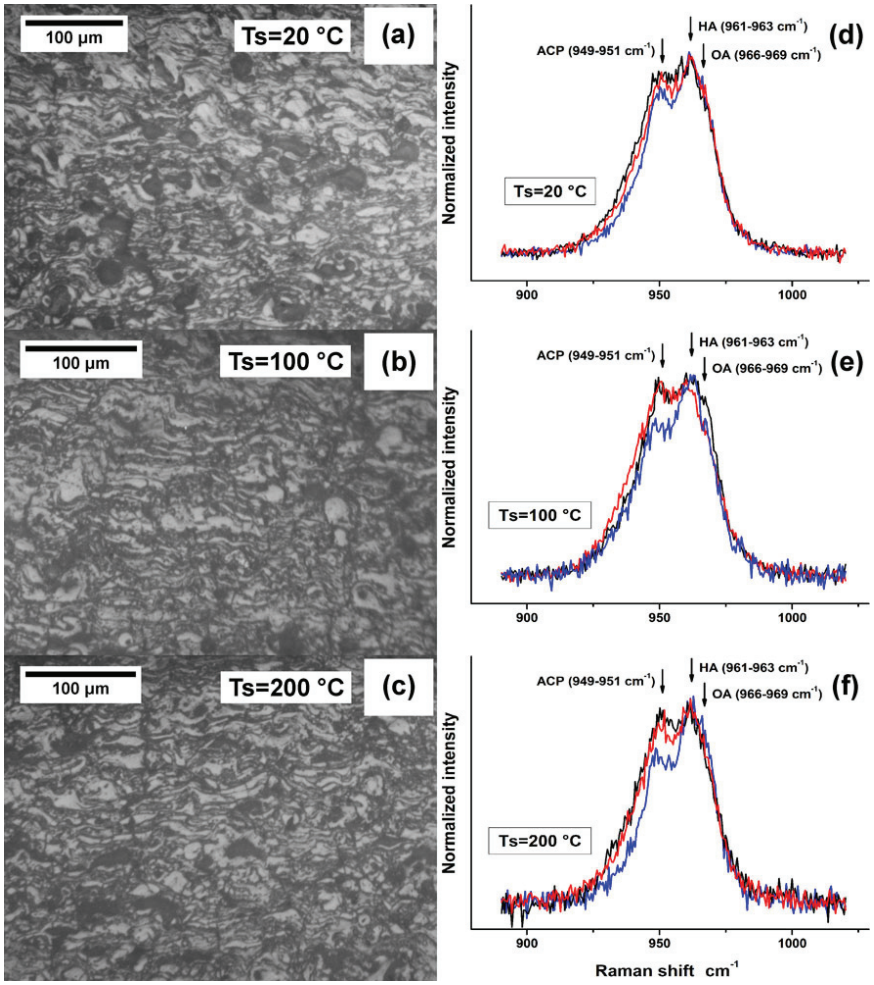

Figure 5. Chemically etched cross-sections of HACs deposited at T_S = 20 (a), 100 (b) and 200 °C (c) and corresponding MRS spectra (d–f).

when substrate preheating was employed. This result is in accordance with the results of Saber-Samandari [8].

In general, the preheating of substrate enables a wider spreading of HA splats on the surface of the substrate or prior-formed HA deposit and, thus, the formation of thinner HA splats [4,8]. For this reason, a good intersplat contact may be achieved, which leads to a higher cohesion strength of HACs. The last might explain the absence of cracking caused by severe cutting in HACs deposited at higher T_S in the present study. On the other hand, taking into account the brittle nature of ACP phase [4], the recrystallized HA in ACP matrix could be observed as an additional barrier for propagation of micro-cracks. In this regard, the distribution of recrystallized regions (HA), observed at higher T_S (Figure 5b and c), was probably beneficial in terms of cracking resistance.

Figure 5d, e and f show MRS spectra which correspond to micro-structures shown in Figure 5a, b and c, respectively. For each T_S, three MRS spectra are shown. Each Raman spectrum exhibited three Raman bands which were attributed to ACP, HA, and OA [9,14,15]. The frequency ranges for these bands are indicated in Figure 5d–f.

The imperceptible differences in the MRS spectrum appearance indicated that the substrate preheating introduced relatively similar amounts of ACP, HA and OA/OHA in HACs deposited at different T_S (Figure 5d–f). According to LM results (Figure 5a–c), the preheating of substrate affected the local distribution of amorphous and recrystallized regions in HACs due to the formation of thinner splats, but it did not significantly affect the local phase composition of HACs according to MRS results (Figure 5d–f). As shown in the previous study, the preheating of substrate has caused noticeable increase of HA content on the expense of the ACP in the near-interface region of HACs [9]. However, the size of the initial HA feedstock powder has been nearly three times larger compared to the present study. For this reason, the high temperature plasma jet has caused the dehydroxylation of larger HA feedstock powder particles to the lower extent compared to the present study and, consequently, the higher content of hydroxyl groups has been available for recrystallization of ACP into HA [9]. On the other hand, in the present study, the lack of the hydroxyl groups (due to a more extensive dehydroxylation of the initial HA feedstock powder of smaller size) probably inhibited the recrystallization of ACP phase upon impact of molten HA particles into the substrate or preformed HA deposit. Namely, it is known that the recrystallization of ACP into OA requires the energy which is nearly twice as that for the recrystallization into HA [20]. In addition, it is known that the crystallization of OA (and especially HA) from the viscous melt will occur in preference to TCP and TTCP [17]. For these reasons, the preheating of substrate (up to 200 °C) was probably insufficient to cause the noticeable effect on the recrystallization of impurity phases, such as TCP, TTCP and CaO. Regarding the high energy levels needed for recrystallization of impurity phases (TCP, TTCP and CaO) and extremely fast cooling conditions that occur upon impact of molten HA particles into the substrate or preformed HA deposit, it was assumed that higher initial substrate temperatures (T_S>200 °C) might cause the observable differences in contents of these phases.

CONCLUSIONS

In the present study, the SEM-EDS results showed that severe cutting conditions introduced cracking within the as-plasma-sprayed HACs. The cracking was localized within the regions with an increased Ca/P mole ratio (>1.8). The phase composition of these regions was dominantly attributed to the hydroxyl-deficient ACP. Further SEM-EDS analysis showed that the substrate preheating promoted an increased cracking resistance of HACs. In contrast to the absence of micro-cracks in HACs deposited at higher T_S, MRS and EDS analyses implied that the substrate preheating did not cause significant changes in the local phase composition. On the other hand, the LM analysis showed a noticeable thinner HA splats and finer distribution of recrystallized HA regions in HACs deposited at higher T_S. These results implied that the effect of the splat formation mechanism on the resulting distribution of amorphous and recrystallized regions in HACs might play an important role regarding the cracking resistance of as-plasma-sprayed HACs.

Acknowledgements

This study was supported by the Plasma Jet Co., Serbia, and by project TR 34022, which was funded by the Ministry of Education, Science and Technological Development of the Republic of Serbia.

REFERENCES

[1] Y.C. Yang, E. Chang, The bonding of plasma-sprayed hydroxyapatite coatings to titanium: effect of processing, porosity and residual stress, Thin Solid Films **444** (2003) 260–275.

[2] M. Topić, T. Ntsoane, R.B. Heimann, Microstructural characterisation and stress determination in as-plasma sprayed and incubated bioconductive hydroxyapatite coatings, Surf. Coat. Technol. **201** (2006) 3633–3641.

[3] Y.C. Yang, Influence of residual stress on bonding strength of the plasma-sprayed hydroxyapatite coating after the vacuum heat treatment, Surf. Coat. Technol. **201** (2007) 7187–7193.

[4] M.F. Morks, A. Kobayashi, Influence of spray parameters on the microstructure and mechanical properties of gas-

-tunnel plasma sprayed hydroxyapatite coatings, Mater. Sci. Eng., B **139** (2007) 209–215.

[5] C.-W. Yang, T.-M. Lee, T.-S. Lui, E. Chang, Effect of post vacuum heating on the microstructural feature and bonding strength of plasma-sprayed hydroxyapatite coatings, Mater. Sci. Eng., C **26** (2006) 1395–1400.

[6] B.-Y. Chou, E. Chang, Influence of deposition temperature on mechanical properties of plasma-sprayed hydroxyapatite coating on titanium alloy with ZrO_2 intermediate layer, J. Therm. Spray Technol. **12** (2009) 199––207.

[7] M. Vilotijević, P. Marković, S. Zec, S. Marinković, V. Jokanović, Hydroxyapatite coatings prepared by a high power laminar plasma jet, J. Mater. Process. Tech. **211** (2011) 996–1004.

[8] S. Saber-Samandari, K. Alamara, S. Saber-Samandari, Calcium phosphate coatings: morphology, micro–structure and mechanical properties, Ceram. Int. **40** (2014) 563–572.

[9] B.R. Gligorijević, M. Vilotijević, M. Šćepanović, N.S. Vuković, N.A. Radović, Substrate preheating and structural properties of power plasma sprayed hydroxyapatite coatings, Ceram. Int. **42** (2016) 411–420.

[10] L. Sun, C.C. Berndt, C.P. Grey, Phase, structural and microstructural investigations of plasma sprayed hydroxyapatite coatings, Mater. Sci. Eng., A **360** (2003) 70–84.

[11] R.A. Surmenev, A review of plasma-assisted methods for calcium phosphate-based coatings fabrication, Surf. Coat. Technol. **206** (2012) 2035–2056.

[12] R.Z. LeGeros, Biodegradation and Bioresorption of Calcium Phosphate Ceramics, Clin. Mater. **14** (1993) 65–88.

[13] S.W.K. Kweh, K.A. Khor, P. Cheang, Plasma-sprayed hydroxyapatite (HA) coatings with flame-spheroidized feedstock: microstructure and mechanical properties, Biomaterials **21** (2000) 1223–1234.

[14] I. Demnati, M. Parco, D. Grossin, I. Fagoaga, C. Drouet, G. Barykin, C. Combes, I. Braceras, S. Goncalves, C. Rey, Hydroxyapatite coating on titanium by a low energy plasma spraying mini-gun, Surf. Coat. Technol. **206** (2012) 2346–2353.

[15] I. Demnati, M. Parco, D. Grossin, I. Fagoaga, C. Drouet, G. Barykin, C. Combes, I. Braceras, S. Goncalves, C. Rey, Plasma-sprayed apatite coatings: Review of physical–chemical characteristics and their biological consequences, J. Med. Biol. Eng. **34** (2014) 1–7.

[16] K. Fox, P.A. Tran, N. Tran, Recent advances in research applications of nanophase hydroxyapatite, ChemPhysChem. **13** (2012) 2495–2506.

[17] K.A. Gross, V. Gross, C.C. Berndt, Thermal processing of hydroxyapatite for coating production, J. Biomed. Mater. Res. **39** (1998) 580–587.

[18] C. Hesse, M. Hengst, R. Kleeberg, J. Gotze, Influence of experimental parameters on spatial phase distribution in as-sprayed and incubated hydroxyapatite coatings, J. Mater. Sci.: Mater. Med. **19** (2008) 3235–3241.

[19] R.A. Surmenev, A review of plasma-assisted methods for calcium phosphate-based coatings fabrication, Surf. Coat. Technol. **206** (2012) 2035–2056.

[20] K.A. Gross, V. Gross, C.C. Berndt, Thermal Analysis of Amorphous Phases in Hydroxyapatite Coatings, J. Am. Ceram. Soc. **81** (1998) 106–112.

IZVOD

LOM IZAZVAN SEČENJEM PLAZMA SPREJ HIDROKSIAPATITNIH PREVLAKA I NJEGOVA VEZA SA STRUKTURNIM SVOJSTVIMA PREVLAKA NANEŠENIH PRI RAZLIČITIM POLAZNIM TEMPERATURAMA SUBSTRATA

Bojan R. Gligorijević[1], Miroljub N. Vilotijević[2,3], Maja J. Šćepanović[4], Radovan V. Radovanović[5], Nenad A. Radović[6]

[1]Univerzitet u Beogradu, Inovacioni centar Tehnološko-metalurškog fakulteta, Karnegijeva 4, 11120 Beograd, Srbija
[2] Univerzitet u Beogradu, Institut za nuklearne nauke Vinča, Mike Petrovića Alasa 12–14, 11001 Beograd, Srbija
[3]Plasma Jet, Braničevska 29, 11000 Beograd, Srbija
[4]Centar za fiziku čvrstog stanja i nove materijale, Institut za fiziku, Univerzitet u Beogradu, Pregrevica 118, 11080 Zemun, Srbija
[5]Kriminalističko–policijska akademija, Cara Dušana 196, 11080 Zemun, Srbija
[6]Univerzitet u Beogradu, Tehnološko-metalurški fakultet, Katedra za metalurško inženjerstvo, Karnegijeva 4, 11120 Beograd, Srbija

(Naučni rad)

Veliki broj studija je pokazao da je čvrstoća (kohezija i adhezija) hidroksiapatitnih (HA) prevlaka dobijenih primenom plazma sprej postupka od izuzetnog značaja u slučajevima njihovog nanošenja na metalne biomedicinske implantima. Uopšteno, HA prevlake, dobijene ovim postupkom, se formiraju od velikog broja delimično i/ili potpuno istopljenih čestica polaznog HA praha koje se brzo hlade pri udaru u substrat i/ili prethodno formirani depozit. Na osnovu prethodnog, kohezija HA prevlaka će zavisiti od prirode kontakta između individualnih čestica HA depozita nastalih brzim hlađenjem, dok će adhezija zavisiti od prirode kontakta između prvog sloja ovih čestica i substrata. Pored rekristalisane HA faze, pri brzom hlađenju HA kapljica dolazi do formiranja krte amorfne kalcijum fosfatne (ACP) faze. Ukoliko se tokom procesa nanošenja ofomi veći broj susednih dominantno amorfnih individualnih čestica HA depozita, taj deo prevlake bi trebalo da ispoljava minimalni otpor ka rastu prslina, s obzirom na izraženu krtost ACP faze. U ovom radu je ispitana pojava loma u hidroksiapatitnim (HA) prevlakama nakon njihovog podvrgavanja agresivnim uslovima sečenja u pravcu normalnom na interfejs prevlaka/substrat. HA prevlake su nanešene primenom visokoenergetskog laminarnog plazma sprej postupka. Kako bi se izvršila procena uticaja predgrevanja substrata, HA prevlake su nanešene pri različitim polaznim temperaturama substrata (T_S = 20, 100, and 200 °C). Nakon sečenja, poprečni preseci HA prevlaka su analizirani primenom skening elektronske mikroskopije sa energetsko-disperzivnom spektrometrijom (SEM-EDS), mikro-Ramanove spektroskopije (MRS) i svetlosne mikroskopije (SM) u kombinaciji sa hemijskim nagrizanjem. Ove tehnike su primenjene u cilju praćenja promena lokalnog faznog sastava HA prevlaka i morfologije individualnih čestica HA depozita sa inicijalnom temperaturom substrata, nakon čega je vršena korelacija ovih svojstava sa pojavom loma u prevlakama. Rezultati ispitivanja su pokazali da su agresivni uslovi sečenja uslovili pojavu lokalizovanog loma u krtim amorfnim (ACP) oblastima HA prevlaka. Ovaj efekat je posebno bio izražen u HA prevlakama koje su nanešene bez predgrevanja substrata. S druge strane, predrevanje substrata na T_S = 100 °C je uzrokovalo primetno manje prisustvo mikro-prslina u HA prevlakama, dok je predgrevanje na T_S = 200 °C izazvalo skoro potpuno odsustvo mikro-prslina. Pritom, značajnije promene u srednjem lokalnom faznom sastavu nisu detektovane. U HA prevlakama kod kojih je vršeno predgrevanje, individualne čestice depozita su bile tanje, a oblasti rekristalisane HA faze su bile manje i ravnomernije raspodeljene u zapremini HA prevlaka. Ovi rezultati su ukazali na to da su mehanizam formiranja individualnih čestica HA depozita i raspodela amorfnih i rekristalisanih oblasti u zapremini HA prevlaka faktori koji mogu značajno da utiču na otpornost ka lomu kod ove vrste prevlaka.

Ključne reči: Plazma sprej postupak • Hidroksiapatitne prevlake • Lom • Predgrevanje substrata